PAPER

Check for updates

Acid-assisted hydrothermal synthesis of red fluorescent carbon dots for sensitive detection of Fe(III)†

Chunlin Tan, [ID] [ac] Xiuya Su, [ad] Chao Zhou, [a] Baoju Wang, [a] Qiuqiang Zhan*[a] and Sailing He*[ab]

Red-emitting carbon dots (C-dots) were synthesized from *p*-phenylenediamine (*p*-PD) aqueous solution with nitric acid (HNO_3) assistance by hydrothermal reaction at 200 °C for 2 h. *p*-PD aqueous solution can be transferred to C-dots (or poly(*p*-PD)) with (or without) the addition of acid. Different acid systems, such as HNO_3, H_3PO_4 and HF, can directly synthesize red-emitting C-dots, and the fluorescence can be enhanced by increasing the strength of acids. N-CDs, 3.46 nm-average-sized C-dots, prepared in dilute HNO_3, have a quantum yield of 15.8% with unique, excitation-wavelength independent emission in the red region (600 and 680 nm) and a broad visible excitation band. Carboxyl, ester and hydroxyl groups on the C-dots surface directly lead to red emission. N-CDs have a certain selective specificity for Fe^{3+} detection and the linear range is 10–300 nmol L^{-1} with a limit of determination of 1.9 nmol L^{-1}.

1. Introduction

Emerging as a new class of zero-dimensional nano-materials, carbon dots (C-dots) have been widely studied during the past decade. Thanks to their advantages including excellent water solubility, optical stability, unique fluorescence properties, low toxicity, low cost, *etc.*,[1] C-dots can be applied in various fields, such as electrochemical immune-sensors,[2] bio-imaging,[3,4] sensors,[5] photo-catalysis[6] and optoelectronics.[7]

Various synthesis methods have been developed since carbon dots were discovered,[8] and they can be mainly categorized into "top-down" and "bottom-up" routes.[9] This classification is mainly based on carbon sources. The "top-down" route physically decomposes macro carbon materials into smaller and smaller nano materials, while the "bottom-up" route chemically creates C-dots by molecular self-assembly reactions from various small molecular reagents. Most of the "bottom-up" routes are efficient to prepare C-dots on a large scale[10] and the carbon sources are widely available from various natural

products (fruit juice,[11–14] dried grass,[15]*etc.*) and small organic molecules.[16] Because of the complex composition of natural products, the photoluminescence (PL) mechanism for C-dots need further study, and thus small molecular carbon sources have become hot research in recent years.

Isomers of phenylenediamine (PD),*o*-, *m*-, and *p*-PD, had been studied as a new carbon source for preparing *o*-CDs,[5,17,18] *m*-CDs,[16] and *p*-CDs,[16,19] respectively, among which *o*-PD and *m*-PD are relatively easy to form C-dots, while there is challenge in employing *p*-PD. *p*-PD has been studied and proposed as a carbon source since 2015,[17] and the as-prepared *p*-CDs emit red fluorescence. After that, Ding *et al.*[19] prepared full-colour C-dots from *p*-PD aqueous solution and urea, and utilized a complex separation process of silica gel column chromatography. However, the process of silica gel column chromatograph is laborious and solvent-, time-, and cost-consuming. The disadvantages of low efficiency, low yield, and high cost of the preparation and separation limit the further applications of *p*-CDs. Metal ions, especially for transition metal ions, are toxic and hard to recycle in wastewater, surface water and ground water.[20] Therefore, it is necessary to develop an efficient metal ions sensor.

Herein, we report a one-pot synthesis for red emitting C-dots from *p*-PD in the assistance of acids. Among the different inorganic acids, such as H_3PO_4, HNO_3, and HF *etc.*, HNO_3 were found to be efficient to prepare red C-dots (labelled as N-CDs). These C-dots possess unique optical properties. The as-prepared N-CDs can be directly used as a sensor to detect metal ions, and they are sensitive for Fe^{3+} sensing at a range of 10–300 nmol L^{-1} with the limit of determination (LOD) of 1.9 nmol L^{-1}.

[a] Centre for Optical and Electromagnetic Research, South China Academy of Advanced Optoelectronics, South China Normal University, 510006 Guangzhou, China. E-mail: zhanqiuqiang@m.scnu.edu.cn; sailing@jorcep.org

[b] JORCEP, Department of Electromagnetic Engineering, Royal Institute of Technology, 10044 Stockholm, Sweden

[c] Centre for Editorial and Publishing Research, South China Normal University, 510006 Guangzhou, China

[d] School of Physics and Telecommunication Engineering, South China Normal University, 510006 Guangzhou, China

2. Experimental section

2.1 Experimental materials

p-PD, hexane, and ethyl alcohol were purchased from Aladdin Co., China. The concentrated acids of HNO_3, HF, H_3PO_4 were purchased from Sinopharm Chemical Reagent Co., China. KCl, $CaCl_2$, $Mg(NO_3)_2$, $Al(NO_3)_3$, $Zn(NO_3)_2$, $FeCl_3$, $SnCl_2$, $Pb(NO_3)_2$, $CuCl_2$, $AgNO_3$, $CoCl_2$, $NiCl_2$, $MnCl_2$, $InCl_3$, $Cd(NO_3)_2$ and $Cr(NO_3)_2$, were purchased from Aladdin Ltd., China. All the reagents were used without purification. Deionized (DI) water was used in the whole experimental procedures.

2.2 Synthesis of CDs

Several parameters, such as different acids, molar ratio of $c(acid):c(p\text{-}PD)$, reaction temperature (T), reaction time (t), were concerned to optimize the experimental conditions. Firstly, mixture aqueous solutions of 0.1 mol L^{-1} p-PD and acid solution (HNO_3, H_3PO_4 or HF) with controlled concentration of x mol L^{-1} were sealed into Teflon-lined autoclave, heated up to 200 °C inside a constant temperature oven keeping for 2 h, and then naturally cooled to room temperature. The $c(acid)$ for the brightest and reddest C-dots under 365 nm UV light (PL assessment, see Fig. S1†) was optimized. Secondly, solutions with y mol L^{-1} p-PD and $c(acid)$ acid were treated as the first step and then the optimal mole ratio was obtained by PL assessment. Thirdly, keeping the optimal mole ratio and other conditions constant and changing $c(p\text{-}PD)$ from 0.02 to 0.20 mol L^{-1}, then the optimal ratio was refined and the range of $c(p\text{-}PD)$ for the preparation of red C-dots was obtained. At last, fixing the refined ratio and other conditions, the reaction temperature T was varied from 140 °C to 220 °C. Similarly, the reaction time t was also optimized ranging from 2 h to 8 h. The optimized experimental parameters, such as the molar ratio, T and t, were finally confirmed (see Fig. S2†). As a contrast, p-PD aqueous solution (0.1 mol L^{-1}) without acid adding was hydrothermally reacted at 200 °C for 2 h. Samples prepared by p-PD aqueous solutions with HNO_3, H_3PO_4, HF, and without acid adding, were labelled as N-CDs, P-CDs, F-CDs, and Pp-PD, respectively. For the purification (see Table S1†), the crude products of N-CDs were successively washed (by hexane to remove the unreacted p-PD), centrifuged (at 14 000 rpm for 30 min to remove polymer precipitation), and filtered (through a 0.22 μm filter membrane). The final concentration of the obtained N-CDs was determined by weighting the mass the dried powder of the corresponding C-dots solution sample.

2.3 Quantum yield measurements

Quantum yields (QYs) of the C-dots were determined by a relative measurement method.[17,21] Specially, Rhodamine B (QYs = 56% in ethanol) was selected as the reference dye for the emission range of 580–610 nm excited by 365 nm UV light. The QYs was calculated by

$$\phi = \phi' \times \frac{A'}{I'} \times \frac{I}{A} \times \frac{n^2}{n'^2}$$

where ϕ and ϕ' are the QYs of sample and reference dye, I and I' are the integrated emission intensity of the sample and dye, n and n' are the refractive indexes (1.33 for H_2O and 1.36 for ethanol) of sample and dye. A series of C-dots solution samples and the reference dye were prepared with proper concentrations to ensure the light absorbance $A < 0.1$ at 365 nm. The QYs values were then obtained by comparing the integrated PL intensities $vs.$ absorbance curves.

2.4 Characterization

High-resolution TEM (HR-TEM) images were recorded on transmission microscope (JEM-2100HR, JEOL) operating at 200 kV. FT-IR spectra of C-dots solutions were collected using FT-IR spectrometer (IRPrestige-21, SHIMADZU) by use of KRS-5 window slices (mixture of TlBr and TlI). Typically, liquid phases were dropped on one slice and dried. The slice was covered by the other slice and fixed on the testing stand, then the infrared spectra recorded.

2.5 Optical measurements

The fluorescence spectra of C-dots were measured using a fluorescence spectrophotometer (F-2500, HITACHI). UV-Vis absorption spectra were recorded on using UV/VIS/NIR Spectrometer (Lambda 950, Perkin Elmer).

2.6 Detection of metal ions

The fluorescence intensity of the N-CDs sample is concentration dependent and reaches its highest value at 0.1 mg mL^{-1}. Therefore, the concentration of C-dots for metal ions sensing is set up at 0.1 mg mL^{-1}. The as-prepared N-CDs solution (9.6 mg mL^{-1}, pH = 3) was diluted to 0.1 mg mL^{-1} by 0.1 mol L^{-1} HNO_3 solution, and all the metal ion solutions were prepared and diluted step-wise with 0.1 mol L^{-1} HNO_3 solution to the concentrations of interest. Herein, 0.1 mol L^{-1} HNO_3 solution was used for two reasons. The one is intended to build a method of metal ions sensing with purification-free C-dots, and the other is to avoid the hydrolysis of some unstable ions, such as Sn^{2+}, Mn^{2+}, $etc.$

Selective sensing experiments for metal ions were carried out by fluorescence intensity quenching method. Typically, 200 μL of different metal ion solutions (1 μmol L^{-1}) or blank sample (0.1 mol L^{-1} HNO_3 solution) were added into 1800 μL N-CDs solutions (1 mg mL^{-1}) to prepare a serious testing solutions (M^{n+} = 100 nmol L^{-1}, blank = 0 nmol L^{-1}). After incubated at 30 °C for 30 min, fluorescence of all incubated solutions were measured at the same excitation wavelength of 510 nm.

For Fe^{3+} sensing experiments, 1800 μL N-CDs (0.1 mg mL^{-1}) and 200 μL Fe^{3+} (0–10 μmol L^{-1}) were incubated at 30 °C for 30 min prior to fluorescence measurements (excited at 510 nm).

3. Results and discussion

3.1 Red C-dots can be prepared from p-PD in acidic solutions

Massive experiments have been performed to optimize the experimental parameters, and the results show that the reproducibility of the proposed synthesis is very high. The best conditions for the preparation of red emitting C-dots are concluded and shown in

Table 1. The molar ratio of c(acid) : c(p-PD) for HNO_3-, H_3PO_4-, and HF-assisted synthesis are 2.5, 7, and 62.5, respectively. The best temperature (180–200 °C) and the reaction time (2 h) are similar. The QYs of N-CDs is the highest (15.8%) (see Table 1, Fig. S3†). In the HNO_3-assisted synthesis, N-CDs emit blue light at the higher mole ratio range of 3.75 to 5 and red light at a lower range of 3 to 1.5 (see Fig. S2a†). When the ratio was fixed to 2.5, all the N-CDs emit red light at the full range (0.02–0.20 mol L^{-1}) of c(p-PD) (see Fig. 1). It is worth noting that N-CDs emit turquoises and blue light when the reaction time was increased to 6 h and above (see Fig. S2a†). In the H_3PO_3-assisted synthesis, all as-prepared P-CDs emit weak red light and show no colour change (see Fig. S1b†). P-CDs are easy to be prepared at a lower temperature (140 °C). However, in general the PL intensities of P-CDs are all weak. In the HF-assisted synthesis, the preparation of F-CDs is acid-consuming and the PL is rich in colour. At the high ratio of 220–500 (see Fig. S2c†), the as-prepared F-CDs emit blue light. At the lower ratio range of 50–100, the F-CDs emit red light. All the as-prepared C-dots crude products are dark burgundy under day light and emit red under 365 nm UV light (see Fig. S2d†).

3.2 TEM characterization and FT-IR analysis

TEM images of Pp-PD and N-CDs were shown in Fig. 2. There were no C-dots but a large amount of polymer nanosheets

Table 1 The optimized reaction parameters of p-PD aqueous solution with different acid systems and the quantum yields of the C-dots aqueous solutions ($10\times$ diluted from as-prepared products)

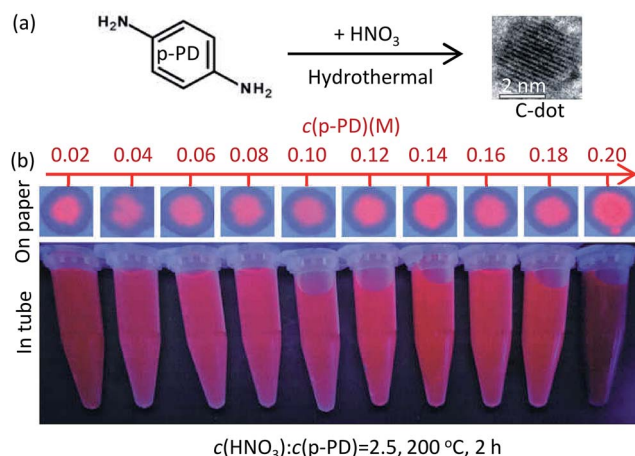| C-dots	Acid	c(acid) (M)	c(p-PD) (M)	T (°C)	t (h)	QYs (%)
F-CDs	HF	10	0.16	200	2	11.5
P-CDs	H_3PO_4	0.7	0.10	180	2	11.7
N-CDs	HNO_3	0.35	0.14	200	2	15.8

Fig. 1 (a) The schematic diagram of N-CDs synthesis. (b) The photographs of PL spots of as-prepared N-CDs aqueous solutions dropped on filter paper (top row) and the N-CDs solutions ($10\times$ diluted from as-prepared products) in tubes (bottom row) under 365 nm UV light.
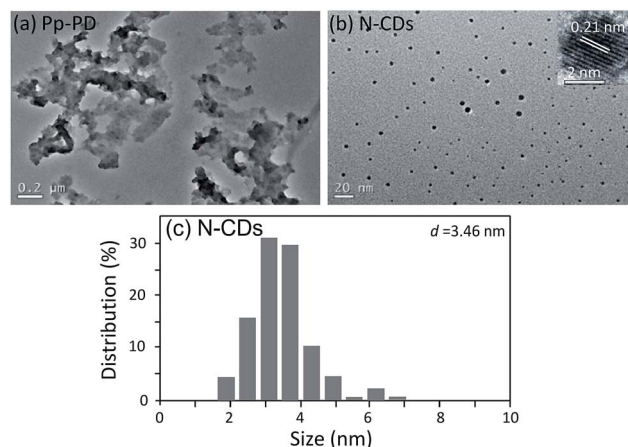

Fig. 2 Reprehensive TEM image of the as-prepared Pp-PD (a) and N-CDs (b), the size distribution of N-CDs (c). The distribution was calculated from the TEM image in (b). N-CDs and Pp-PD were prepared by hydrothermal reaction from p-PD aqueous solution with and without HNO_3 assistance.

formed in the p-PD aqueous solution without acid added (see Fig. 2a), while the red-emitting C-dots formed in the assistance of acids. N-CDs, which were prepared from p-PD with the assistance of HNO_3, are uniform and monodisperse nanodots (see Fig. 2b) with an average diameter of 3.46 nm (see Fig. 2c). The C-dots exhibit identical well-resolved lattice fringes with a space of ~0.21 nm, corresponding to the (100) in-plane lattice spacing of graphene.[22,23] It indicates that the addition of acid can inhibit the polymerization process and promoted the formation of nanodots.

Chemical groups on the surface of C-dots may impact the optical properties. From the FT-IR spectra of N-CDs (see Fig. 3), N-CDs contain many groups derived from the precursor, such as ν(Ar–H) (2700–3200 cm^{-1}, belonging to aromatic C–H stretching vibration[24]), δ(Ar–H) (800–850 cm^{-1}, belonging to aromatic C–H out-of-plane deformation vibration of substituted benzene ring[25]), and δ(N–H) (1520 cm^{-1}, belonging to the deformation vibration of –NH_2 or –NH– groups). Other groups, such as ν(O–H) (3500 cm^{-1}, belonging to the deformation vibration of –OH groups in aliphatic alcohols), ν(C=O) (1600 cm^{-1}, belonging to the stretching vibration of carbonyl in carboxyl groups), and ν(C–O–C) (1200 cm^{-1}, belonging to the stretching vibration of
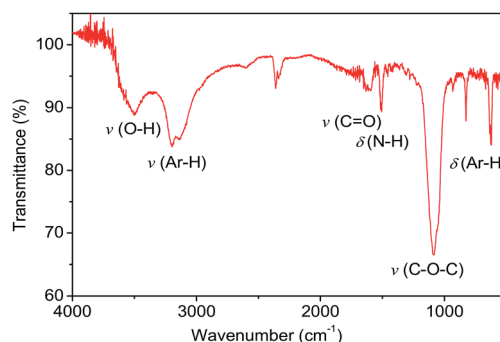

Fig. 3 FT-IR spectra of N-CDs prepared from p-PD and HNO_3 solution.

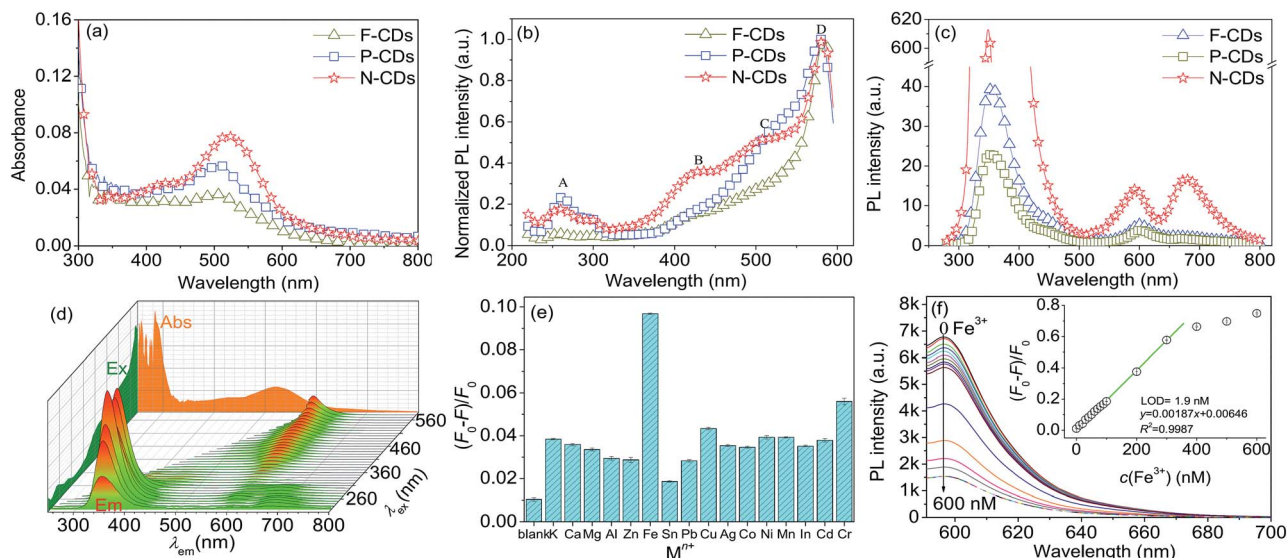**Fig. 4** UV-Vis absorption (a), excitation (λ_{em} = 600 nm) (b) and emission (λ_{ex} = 260 nm) spectra (c) of different C-dots aqueous solutions (10× diluted from as-prepared products), the emission spectra of N-CDs aqueous solution (10× diluted from the as-prepared product) with the λ_{ex} = 260–580 nm (d), the selectivity (e) and the sensitivity (f) of N-CDs (0.1 mg mL^{-1}) for the Fe^{3+} ions sensing in 0.1 mol L^{-1} HNO$_3$ solutions. The concentrations of metal ions are all at 100 nmol L^{-1} (e), and the Fe^{3+} concentrations varied at 0, 10, 20, 30, 40, 50, 60, 70, 80, 90, 100, 200, 300, 400, 500, and 600 nmol L^{-1} (f). Fluorescence curves of all the samples were measured at the excitation wavelength of 510 nm. The inset in (f) is the linearity of PL intensity at 580 nm against the measured Fe^{3+} concentrations.

ester groups), were formed by ring opening and oxidation reactions.

3.3 Optical properties

Although being prepared assisted with different acids, F-CDs, P-CDs and N-CDs showed similar optical properties (see Fig. 4). For UV-Vis spectra, the absorption peaks are located at around 290 and 510 nm, and the absorbance intensities are relatively strong at the range from UV to visible light zone (350–600 nm, see Fig. 4a). The maximum wavelengths of the absorption peaks at around 510 nm occurred red-shift in the order of F-CDs, P-CDs, and N-CDs, this is due to the gradually increasing of acidity and oxidation of acids that added in the precursors. For excitation, there are 4 obvious peaks (A: 260 nm, B: 430 nm, C: 510 nm and D: 580 nm) in N-CDs while several peaks are less prominent in F-CDs and P-CDs samples, and all CDs can be excited at a maximum wavelength of 580 nm (see Fig. 4b). It indicates that N-CDs have a broad and efficient excitation band in the visible region. For emission, being excited at the same wavelength (260 nm), F-CDs and P-CDs emit at 355 and 600 nm, while N-CDs emission slightly blue-shift (349 and 594 nm) and another significant peak is found at around 680 nm (see Fig. 4c). This 680 nm-peak can increase the intensity of red light emission for N-CDs. N-CDs is more chemically stable than P-CDs and F-CDs. It is worth noting that the emission is excitation-wavelength-independent (see Fig. 4d).[26] This indicates that N-CDs are homogeneous C-dots and emit at a single dot level.[27–29]

3.4 Selective Fe(III) sensing

The selectivity results of N-CDs for 16 kinds of different metal ions are shown in Fig. 4e. Among the tested metal ions, Fe^{3+} is

relatively efficient to quench the PL of N-CDs. Fe^{3+} sensing experiments by using N-CDs probe were carried out as Fig. 4f. The quenching of N-CDs is linear at the range of 10–300 nmol L^{-1} of Fe^{3+}, and the LOD is 1.9 nmol L^{-1}.

C-dots were environmental friendly and potential alternative of fluorescent dyes in metal ions detection. The most prominent advantage is that the red-emitting C-dots can be excited at visible region (400–580 nm) and avoid the use of UV light.

4. Conclusions

p-Phenylenediamine (p-PD) aqueous solution can be transformed to C-dots (or poly(p-PD)) with (or without) acid assistance. Many common inorganic acid, such as HNO$_3$, H$_3$PO$_4$ and HF, can efficiently help to synthesize red-emitting C-dots. The red-emission of p-PD-based C-dots can be enhanced by strong acid (such as HNO$_3$). N-CDs, prepared with the assistance of HNO$_3$, have a wide linear range with a lower LOD for Fe^{3+} sensing. The selectivity could be further improved for future applications. QYs and the selectivity are two key challenges for N-CDs applied in metal ions detection. Introducing the third reactants, which contain amino- and carboxylic-groups, will be our further research work. Red-emitting C-dots would be also very powerful in the biomedical optical imaging and sensing.

Conflicts of interest

There are no conflicts to declare.

Acknowledgements

References

1 N. Durán, M. B. Simões, A. C. M. de Moraes, W. J. Fávaro and A. B. Seabra, *J. Biomed. Nanotechnol.*, 2016, **12**, 1323.

2 T. S. Xu, X. Y. Li, Z. H. Xie, X. G. Li and H. Y. Zhang, *Microchim. Acta*, 2015, **182**, 2541.

3 J. C. Ge, Q. Y. Jia, W. M. Liu, L. Guo, Q. Y. Liu, M. H. Lan, H. Y. Zhang, X. M. Meng and P. F. Wang, *Adv. Mater.*, 2015, **27**, 4169.

4 L. Bao, C. Liu, Z. L. Zhang and D. W. Pang, *Adv. Mater.*, 2015, **27**, 1663.

5 M. Vedamalai, A. P. Periasamy, C. W. Wang, Y. T. Tseng, L. C. Ho, C. C. Shih and H. T. Chang, *Nanoscale*, 2014, **6**, 13119.

6 S. L. Hu, Z. J. Wei, Q. Chang, A. Trinchi and J. L. Yang, *Appl. Surf. Sci.*, 2016, **378**, 402.

7 P. Mirtchev, E. J. Henderson, N. Soheilnia, C. M. Yip and G. A. Ozin, *J. Mater. Chem.*, 2011, **22**, 1265.

8 X. Y. Xu, R. Ray, Y. L. Gu, H. J. Ploehn, L. Gearheart, K. Raker and W. A. Scrivens, *J. Am. Chem. Soc.*, 2004, **126**, 12736.

9 S. N. Baker and G. A. Baker, *Angew. Chem., Int. Ed.*, 2010, **49**, 6726.

10 S. J. Zhu, Y. B. Song, X. H. Zhao, J. R. Shao, J. H. Zhang and B. Yang, *Nano Res.*, 2015, **8**, 355.

11 J. Yu, N. Song, Y. K. Zhang, S. X. Zhong, A. J. Wang and J. R. Chen, *Sens. Actuators, B*, 2015, **214**, 29.

12 Y. Liu, Y. N. Liu, M. Park, S. J. Park, Y. F. Zhang, M. R. Akanda, B. Y. Park and H. Y. Kim, *Carbon Lett.*, 2017, **21**, 61.

13 B. S. B. Kasibabu, S. L. D'souza, S. Jha and S. K. Kailasa, *J. Fluoresc.*, 2015, **25**, 803.

14 V. N. Mehta, S. Jha and S. K. Kailasa, *Mater. Sci. Eng., C*, 2014, **38**, 20.

15 H. Zhang, Y. Wang, D. Wang, Y. B. Li, P. Liu, H. G. Yang, T. C. An, Z. Y. Tang and H. J. Zhao, *Small*, 2014, **10**, 3371.

16 Y. W. Zheng, D. Yang, X. Wu, H. R. Yan, Y. C. Zhao, B. Feng, K. Duan, J. Weng and J. X. Wang, *RSC Adv.*, 2015, **5**, 90245.

17 K. Jiang, S. Sun, L. Zhang, Y. Lu, A. G. Wu, C. Z. Cai and H. W. Lin, *Angew. Chem., Int. Ed.*, 2015, **54**, 5360.

18 L. Song, Y. Y. Cui, C. F. Zhang, Z. B. Hu and X. F. Liu, *RSC Adv.*, 2016, **6**, 17704.

19 H. Ding, S. B. Yu, J. S. Wei and H. M. Xiong, *ACS Nano*, 2016, **10**, 484.

20 P. Wang, P. Y. Xiao, S. X. Zhong, J. R. Chen, H. J. Lin and X. L. Wu, *J. Mater. Chem. A*, 2016, **4**, 15450.

21 M. Grabolle, M. Spieles, V. Lesnyak, N. Gaponik, A. Eychmüller and U. Reschgenger, *Anal. Chem.*, 2009, **81**, 6285.

22 S. Qu, D. Zhou, D. Li, W. Ji, P. Jing, D. Han, L. Liu, H. Zeng and D. Shen, *Adv. Mater.*, 2016, **28**, 3516.

23 L. Tang, R. Ji, X. Li, G. Bai, C. P. Liu, J. Hao, J. Lin, H. Jiang, K. S. Teng and Z. Yang, *ACS Nano*, 2014, **8**, 6312.

24 Z. Gao, Z. Lin, X. Chen, H. Zhong and Z. Huang, *Anal. Methods*, 2016, **8**, 2297.

25 A. M. Craciun, A. Diac, M. Focsan, C. Socaci, K. Magyari, D. Maniu, I. Mihalache, L. M. Veca, S. Astilean and A. Terec, *RSC Adv.*, 2016, **6**, 56944.

26 Z. H. Wen and X. B. Yin, *RSC Adv.*, 2016, **6**, 27829.

27 S. Ghosh, A. M. Chizhik, N. Karedla, M. O. Dekaliuk, I. Gregor, H. Schuhmann, M. Seibt, K. Bodensiek, I. A. T. Schaap, O. Schulz, A. P. Demchenko, J. Enderlein and A. I. Chizhik, *Nano Lett.*, 2014, **14**, 5656.

28 V. Strauss, J. T. Margraf, C. Dolle, B. Butz, T. J. Nacken, J. Walter, W. Bauer, W. Peukert, E. Spiecker, T. Clark and D. M. Guldi, *J. Am. Chem. Soc.*, 2014, **136**, 17308.

29 S. K. Das, Y. Liu, S. Yeom, D. Y. Kim and C. I. Richards, *Nano Lett.*, 2014, **14**, 620.